J Ginseng Res 43 (2019) 196–208

Contents lists available at ScienceDirect

Journal of Ginseng Research

journal homepage: http://www.ginsengres.org

Research Article

Fermented ginseng, GBCK25, ameliorates steatosis and inflammation in nonalcoholic steatohepatitis model

Naeun Choi [1,☆], Jong Won Kim [1,☆], Hyeneui Jeong [1], Dong Gue Shin [2], Jeong Hun Seo [2], Jong Hoon Kim [1], Chae Woong Lim [1], Kang Min Han [3,**], Bumseok Kim [1,*]

[1] Biosafety Research Institute and Laboratory of Pathology (BK21 Plus Program), College of Veterinary Medicine, Chonbuk National University, Iksan, Republic of Korea
[2] Research & Development Center of GENERAL BIO Co., Ltd, Namwon City, Jeollabuk-Do, Republic of Korea
[3] Department of Pathology, Dongguk University Ilsan Hospital, Goyang, Republic of Korea

ARTICLE INFO

Article history:
Received 3 July 2017
Received in Revised form
27 September 2017
Accepted 13 October 2017
Available online 21 October 2017

Keywords:
compound K
cytochrome P450 2E1
ginseng
mice
nonalcoholic steatohepatitis

ABSTRACT

Background: Nonalcoholic steatohepatitis (NASH) is one of the chronic inflammatory liver diseases and a leading cause of advanced liver fibrosis, cirrhosis, and hepatocellular carcinoma. The main purpose of this study was to clarify the effects of GBCK25 fermented by *Saccharomyces servazzii* GB-07 and pectinase, on NASH severity in mice.

Methods: Six-wk-old male mice were fed either a normal diet (ND) or a Western diet (WD) for 12 wks to induce NASH. Each group was orally administered with vehicle or GBCK25 once daily at a dose of 10 mg/kg, 20 mg/kg, 100 mg/kg, 200 mg/kg, or 400 mg/kg during that time. The effects of GBCK25 on cellular damage and inflammation were determined by *in vitro* experiments.

Results: Histopathologic analysis and hepatic/serum biochemical levels revealed that WD-fed mice showed severe steatosis and liver injury compared to ND-fed mice. Such lesions were significantly decreased in the livers of WD-fed mice with GBCK25 administration. Consistently, mRNA expression levels of NASH-related inflammatory-, fibrogenic-, and lipid metabolism-related genes were decreased in the livers of WD-fed mice administered with GBCK25 compared to WD-fed mice. Western blot analysis revealed decreased protein levels of cytochrome P450 2E1 (CYP2E1) with concomitantly reduced activation of c-Jun N-terminal kinase (JNK) in the livers of WD-fed mice administered with GBCK25. Also, decreased cellular damage and inflammation were observed in alpha mouse liver 12 (AML12) cells and RAW264.7 cells, respectively.

Conclusion: Administration of GBCK25 ameliorates NASH severity through the modulation of CYP2E1 and its associated JNK-mediated cellular damage. GBCK25 could be a potentially effective prophylactic strategy to prevent metabolic diseases including NASH.

1. Introduction

The more advanced and severe form of nonalcoholic fatty liver disease (NAFLD) is called nonalcoholic steatohepatitis (NASH). NASH is a prevalent liver disease worldwide and is considered a major cause of advanced fibrosis, cirrhosis, and hepatocellular carcinoma [1,2]. Recently, NAFLD and/or NASH have become increasingly prevalent because of overnutrition combined with lack of exercise. As well as having the potential to develop into end-stage liver disease, NAFLD and/or NASH are closely associated with several nonhepatic or systemic complications [3]. Major risk factors for their development include rich diet, obesity, insulin resistance (IR), glucose intolerance, and dyslipidemia [4].

* Corresponding author. Biosafety Research Institute and Laboratory of Pathology (BK21 Plus Program), College of Veterinary Medicine, Chonbuk National University, 79, Gobong-ro, Iksan 54596, Republic of Korea.
** Corresponding author. Department of Pathology, Dongguk University Ilsan Hospital, 27, Dongguk-ro, Goyang 10326, Republic of Korea.
E-mail addresses: Kiekie53@dumc.or.kr (K.M. Han), bskims@jbnu.ac.kr (B. Kim).
☆ N. Choi and J.W. Kim contributed equally to this work.

https://doi.org/10.1016/j.jgr.2017.10.002
p1226-8453 e2093-4947/$ – see front matter

One of the common features in patients with IR or NASH is increased oxidative stress [5]. Therefore, oxidative stress is known to be as one of the pathogenic factors that expedite the progression from steatosis to steatohepatitis [6]. Overproduction of mitochondria-derived reactive oxygen species (ROS) are involved in increasing the burden of oxidative stress leading to hepatocellular damage. Also, ROS could increase levels of lipid peroxides, which form adducts with intracellular components. Consequently, formation of these adducts results in cellular damage and a subsequent induction of inflammatory response [7,8]. In the cytochrome P450 family, cytochrome P450 2E1 (CYP2E1) is closely associated with the pathogenesis of NAFLD and/or NASH. It has been understood that CYP2E1-mediated ROS generation and consequent oxidative stress play pivotal roles in progression of both alcoholic and nonalcoholic steatohepatitis [9,10]. Therefore, several cancers and liver diseases are involved in genetic variation in CYP2E1 [11–13]. Although several human studies have investigated the genetic diversity of CYP2E1 in patients with NAFLD, the correlation between CYP2E1 variants and susceptibility to NASH remains undetermined [14,15].

Ginseng root is the basis of traditional and alternative medicines that have been widely used in Asia for thousands of years [16]. The ginsenoside constituents have been reported to exhibit various pathophysiologic activities, including anti-inflammatory activity and antitumor effects mediated by inhibiting tumor-induced angiogenesis, tumor invasion, and metastasis [17]. Recently, it was reported that Korean Red Ginseng ameliorates the severity of NAFLD by reducing inflammatory responses and oxidative stress [18,19]. Moreover, compound K (CK), a final metabolite of panaxadiol ginsenosides, has received a great deal of attention in recent years because of its prophylactic activities against several diseases including atherosclerosis [20] and several cancers including hepatocellular carcinoma [21]. CK also has suppressive effects on acute liver injury induced by acetaminophen overdose [22] or *tert*-butyl hydroperoxide injection [23]. As well as having protective roles for acute hepatotoxic injury, CK has beneficial effects on metabolic disorder-related liver diseases through the reduction of hepatocellular lipid accumulation and hepatic gluconeogenesis, and by reducing the glucose intolerance caused by the activation of adenosine 5′-monophosphate kinase-dependent pathway [24–26]. Furthermore, administration of CK alleviates hepatic fibrogenic responses and impaired liver function induced by a high fat diet (HFD) [27]. However, the role of CK on NASH development and/or progression remains unclear.

Therefore, the aim of our study was to determine the effects of ginseng (GBCK25) fermented by a novel *Saccharomyces servazzii* strain, GB-07, using pectinase on NASH severity in mice.

2. Materials and methods

2.1. GBCK25 ingredient inspection

The amount of ginsenosides from GBCK25; 18.71 mg/g of ginsenoside -Rg1, 43.51 mg/g -Re, 40.45 mg/g -Rh1(s)+Rg2(s), 18.73 mg/g -Rb2, 10.23 mg/g -Rd, 4.36 mg/g -Rg3(s), 23.32 mg/g -CK and other minor of contents (Fig. 1).

2.2. Animals and experimental protocol

Male 6-wk-old C57BL/6 wild-type mice were purchased from Samtako Bio Korea (O-San, South Korea) and used in this study. The mice were housed under a standard condition (24 ± 3°C, 50 ± 5% humidity) and were fed sterile normal diet (ND) and water *ad libitum*. Experimental and animal management procedures were officially approved by the Animal Care and Ethics Committees of Chonbuk National University. GBCK25 was obtained from GENERAL BIO Co. Ltd. (Wanju-gun, Korea). After an adaptation period, mice were separated into seven groups: (1) mice receiving ND ($n = 10$); (2) mice receiving Western diet (WD; high in fat (40 kcal%), fructose (20 kcal%), and 2% cholesterol, $n = 10$, CK 0); (3) mice receiving WD with GBCK25 at 10 mg/kg/d ($n = 9$, CK 10), 20 mg/kg/d ($n = 10$, CK 20), 100 mg/kg/d ($n = 9$, CK 100), 200 mg/kg/d ($n = 12$, CK 200), or 400 mg/kg/d ($n = 10$, CK 400). GBCK25 was dissolved in distilled water through sonication, and was orally administered once daily for 12 wks in each WD diet-fed group.

2.3. Histopathologic analysis

After tissue fixing with 10% neutral buffered formalin solution, liver tissues were finally embedded in paraffin using standard protocol. Tissue sections (6 μm) were prepared using HM-340E microtome (Thermo Fisher Scientific Inc., Waltham, MA, USA), and stained with hematoxylin and eosin (H&E) according to standard methods. Histopathological analysis of liver sections was performed using light microscopy (BX-51 microscope; Olympus Corp., Tokyo, Japan).

2.4. NAFLD activity score

To confirm NASH severity, H&E-stained liver sections were evaluated by NAFLD activity score (NAS) scoring system according to previous reports [28]. This system considered the degree of steatosis (0–3), lobular inflammation (0–3), and ballooning degeneration of hepatocytes (0–2). The sum of these scores, NAS, indicated the severity of NAFLD and/or NASH.

2.5. Oil Red O staining

The Oil Red O stain kit (Scytek Lab., Logan, UT, USA) was used to measure lipid accumulation in hepatocytes according to the manufacturer's instruction. Briefly, frozen liver sections were washed with propylene glycol for 5 min at room temperature, stained with heated (60°C) Oil Red O solution for 20 min, and counterstained with hematoxylin for 1 min. Data are expressed as percentages of the Oil Red O-positive area per field analyzed by using a light microscope and digital image software (analySIS TS; Olympus Corp.).

2.6. Serum and hepatic biochemical measurements

Liver injury was evaluated by measuring serum levels of aspartate aminotransferase (AST) and alanine aminotransferase (ALT) determined by AM101-K spectrophotometric assay kits (ASAN Pharmaceutical, Hwasung, Korea). Hepatic lipid accumulation was assessed by measuring triglyceride (TG) and total cholesterol (TC) contents with an AM202-K spectrophotometric assay kit (ASAN Pharmaceutical). The absorbance of samples was quantified at a wavelength of 490 nm or 550 nm using an EMax spectrophotometer (Molecular Devices, Sunnyvale, CA, USA).

2.7. Quantitative real time-polymerase chain reaction

RNA was extracted from liver tissue using the Hybrid-R RNA purification kit (GeneAll Biotechnology Co. Ltd., Seoul, Korea). Following incubation with DNase I containing RNase inhibitor (TOYOBO, Osaka, Japan), samples were transcribed using ReverTra Ace qPCR RT Master Mix (TOYOBO) according to the manufacturer's instructions. Quantitative real time-polymerase chain reaction (qRT-PCR) was performed in the CFX96 Real-Time PCR Detection System (Bio-Rad Laboratories, Hercules, CA, USA) using SYBR Green (TOYOBO). After the reaction was complete, specificity was verified

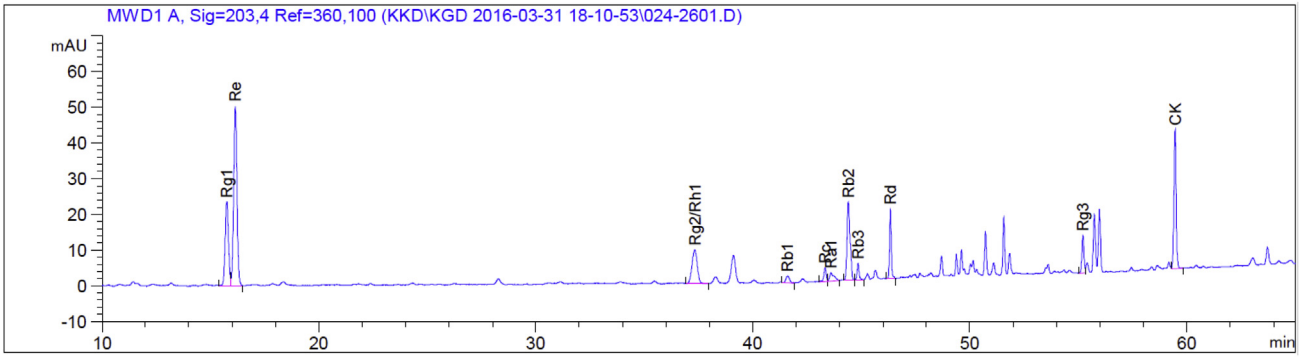

Fig. 1. Ingredient inspection of GBCK25. Representative picture showing high performance liquid chromatography analysis of GBCK25.

by melting curve analysis. Relative quantification was performed by normalizing to the value of ribosomal protein lateral stalk subunit P0 (RPLP0). The primer sequences are shown in Table 1.

2.8. Cell culture, Kupffer cell isolation, and GBCK25 treatment

The alpha mouse liver 12 (AML12) cell line was kindly provided by Professor Heungsik Choi, Chonnam National University (Gwangju, Korea). AML12 cells were cultured in Dulbecco's modified Eagle's medium (DMEM)/F12 (WELGENE Inc., Gyeongsan-si, Korea) including 10% fetal bovine serum (WELGENE Inc.), Insulin–Transferrin–Selenium–Pyruvate supplement solution (WELGENE Inc.), 40 ng/mL of dexamethasone (Sigma–Aldrich, St, Louis, MO, USA), 100 IU/mL penicillin, and 100 μg/mL streptomycin (WELGENE Inc.) at 37°C in a 5% CO_2 incubator. For *in vitro* experiments, cells were incubated overnight in serum-free medium. Following incubation, cells were stimulated with palmitic acid (PA; 0.5mM; Sigma–Aldrich) or together with treatment of GBCK25 (1 μg/mL, 2 μg/mL, and 4 μg/mL) for 24 h. Murine monocyte/macrophage cell line RAW264.7 was obtained from the American Type Culture Collection (Rockville, MD, USA) and cultured at 37°C under 5% CO_2 in DMEM (WELGENE Inc.) including 10% fetal bovine serum, 100 IU/mL penicillin, and 100 μg/mL streptomycin (WELGENE Inc.). For *ex vivo* experiments, primary Kupffer cells (KCs) were isolated as previously described [29]. Briefly, mouse livers were digested by collagenase (1 mL/min) perfusion followed by two-layer discontinuous density gradient centrifugation with 70% and 40% Percoll (Sigma–Aldrich). Cells were collected from the interface, and KCs were positively selected by magnetic cell sorting using anti-F4/80 antibody (Miltenyi Biotech, Auburn, CA, USA). Cells were stimulated by treatment of 1 μg/mL lipopolysaccharide (LPS; Sigma–Aldrich) or together with treatment of GBCK25 (0.3 μg/mL, 0.4 μg/mL, or 0.5 μg/mL) for 24 h.

Table 1
Primer sequence of genes used for quantitative real time-polymerase chain reaction (qRT-PCR)

Gene	Forward	Reverse
TNF-α	GTCTACTCCCAGGTTTCTCTTCAAGG	GCAAATCGGCTGACGGTGTG
IL-1β	CTCGCAGCAGCACATCAACA	CCACGGGAAAGACACAGGTA
IL-6	CAACGATGATGCACTTGCAGA	CTCCAGGTAGCTATGGTACTCCAGA
Col 1α	ACAGGCGAAACCGGTGACAG	GCCAGGAGAACCAGCAGAGC
α-SMA	TCAGGGAGTAATGGTTGGAA	CAGTTGGTGATGATGCCGTG
TGF-β	TGAACCAAGGAGACGGAATACAGG	GCCATGAGGAGCAGGAAGGG
TIMP-1	TCTGGCATCTGGCATCCTCTTG	AACGCTGGTATAAGGTGGTCTCG
ACCα	CAAGCCCGTGAGAACACAG	GAGTGTGTTTGACCAGGAACAATGA
FAS	GGGTCGTTTCTCCATTAAATTCTCAT	CTAGAAACTTTCCCAGAAATCTCC
DGAT1	GCTCAGACAGTGGTTTCAGCAATTA	ACAGAGACACCACCTGGATAGGA
ApoB	TCCTCGGTGAGTTCAATGACTTTC	TGGACCTGCTGTAGCTTGTAGGA
MTTP	CATCTCCACAGTGCAGTTCTCACA	GGAGTTCACATCCGGCCACTA
CPT1	GATCAATCGGACCCTAGACAC	AGAGCAGCACCTTCAGCGAGTA
CYP2E1	AAGCGCTTCGGGCCAG	TAGCCATGCAGGACCACGA
CYP3A11	CGCCTCTCCTTGCTGTCACA	CTTTGCCTTCTGCCTCAAGT
CYP4A10	GAGTGTCTCTGCTCTAAGCCCA	AGGCTGGGGTTAGCATCCTCCT
RpLp0	CCACACTGCTGAACATGCTGAA	GTACCCGATCTGCAGACACACAC

ACCα, acetyl CoA carboxylase α; ApoB, apolipoprotein B; αSMA, alpha smooth muscle actin; Col 1α, type I collagen alpha 1; CPT1, carnitine palmitoyltransferase 1; CYP2E1, cytochrome P450 2E1; DGAT1, diacylglycerol *O*-acyltransferase 1; FAS, fatty acid synthase; IL-1β, interleukin-1 beta; IL-6, interleukin-6; MTTP, microsomal triglyceride transfer protein; RpLp0, ribosomal protein lateral stalk subunit P0; TGF-β, transforming growth factor-beta; TIMP-1, tissue inhibitor of metalloproteinase-1; TNF-α, tumor necrosis factor-alpha

2.9. Cell viability assay

Cells were seeded in a 96-well plate (1×10^4 cells/well) and allowed to adhere in serum-free medium for 24 h. After 24 h, cells were treated with indicated concentration of GBCK25 for 24 h, and then cell viability was measured using the CellTiter 96® AQueous One Solution Cell Proliferation Assay (Promega, Madison, WI, USA). The absorbance of samples was quantified at 490 nm using the aforementioned spectrophotometer.

2.10. In vitro cellular TG measurement

To measure the levels of cellular TG, cells were seeded in wells of a 96-well plate and then cultured in the presence of PA with or without GBCK25 treatment as described above. After 24 h incubation, the medium was removed and cells were washed several times with phosphate buffered saline. Following complete removal of phosphate buffered saline, 10 μL dimethyl sulfoxide was added for 1 min to extract intracellular TG in each well. The levels of cellular TG were determined using an aforementioned commercial kit according to the manufacturer's instructions. The absorbance of samples was quantified at the wavelength of 550 nm using the aforementioned EMax spectrophotometer.

2.11. Malondialdehyde assay

To estimate lipid peroxidation in liver tissues, thiobarbituric acid reactive substances (TBARS) in the form of malondialdehyde (MDA) were measured using an OxiSelect TBARS Assay Kit (Cell Biolabs, Inc., San Diego, CA, USA).

2.12. Western blot assay

Liver tissues or cells were directly lysed for 30 min on ice with an extraction buffer (T-PER or RIPA; Thermo Fisher Scientific Inc.). Protein concentration was determined using Pierce BCA Protein Assay kit (Thermo Fisher Scientific Inc.) according to the

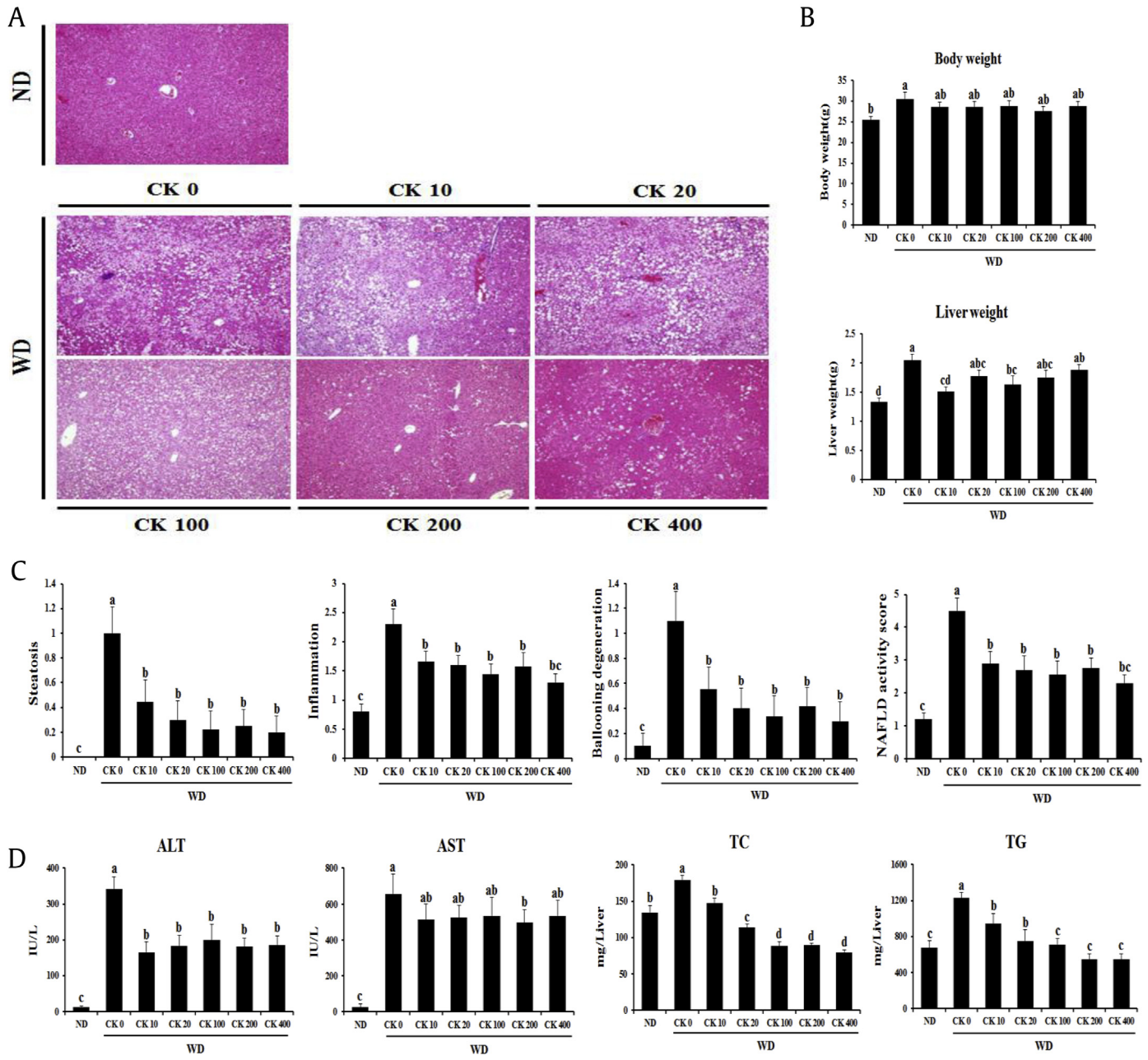

Fig. 2. GBCK25 administration affects NASH progression. (A) Representative pictures showed H&E-stained liver sections at 100× magnification. (B) Body weight and liver weight were measured. (C) NAFLD activity score was evaluated. (D) Serum and hepatic biochemical were determined to evaluate NASH-related liver injury and lipid accumulation. Statistically significant difference between groups is indicated with different letters (mean ± SEM, ANOVA, $p < 0.05$). ALT, alanine aminotransferase; ANOVA, analysis of variance; AST, aspartate aminotransferase; CK, compound K; H&E, hematoxylin and eosin; NAFLD, nonalcoholic fatty liver disease; NASH, nonalcoholic steatohepatitis; ND, normal diet; SEM, standard error of the mean; TC, total cholesterol; TG, triglyceride; WD, Western diet.

manufacturer's protocol. Following sodium dodecyl sulfate–polyacrylamide gel electrophoresis, gels were transferred to a polyvinylidene difluoride membrane, and then blocked with 5% bovine serum albumin in Tris-buffered saline (20mM Tris, 150mM NaCl, pH 7.4) with 0.05% Tween-20 for 1 h at room temperature. Primary antibodies were diluted at 1:1,000 in blocking solution and incubated overnight at 4°C. Antibodies specific for CYP2E1 (Abcam, Cambridge, UK), c-Jun N-terminal kinase (JNK), phospho JNK (pJNK), and β-actin (Cell Signaling Technology, Danvers, MA, USA) were used. Secondary horseradish peroxidase-conjugated IgG antibodies (Santa Cruz Biotechnology Inc., Santa Cruz, CA, USA) were used to detect antigen–antibody complexes on polyvinylidene difluoride membranes. Immunoblot images were visualized with ImageQuant LAS 500 (GE Healthcare Life Science, Pittsburgh, PA, USA). The expression levels of protein bands were quantified with ImageQuant TL software (GE Healthcare Life Science).

2.13. Enzyme-linked immunosorbent assay

To measure hepatic inflammatory cytokines, hepatic protein was extracted according to the above-mentioned protocol. The protein levels of tumor necrosis factor-alpha (TNF-α), interleukin-6 (IL-6), and IL-1 beta (IL-1β) were measured using enzyme-linked immunosorbent assay (ELISA) kits (e-Bioscience, San Diego, CA, USA) according to the manufacturer's instructions. Absorbance at 450 nm was measured using the aforementioned EMax spectrophotometer.

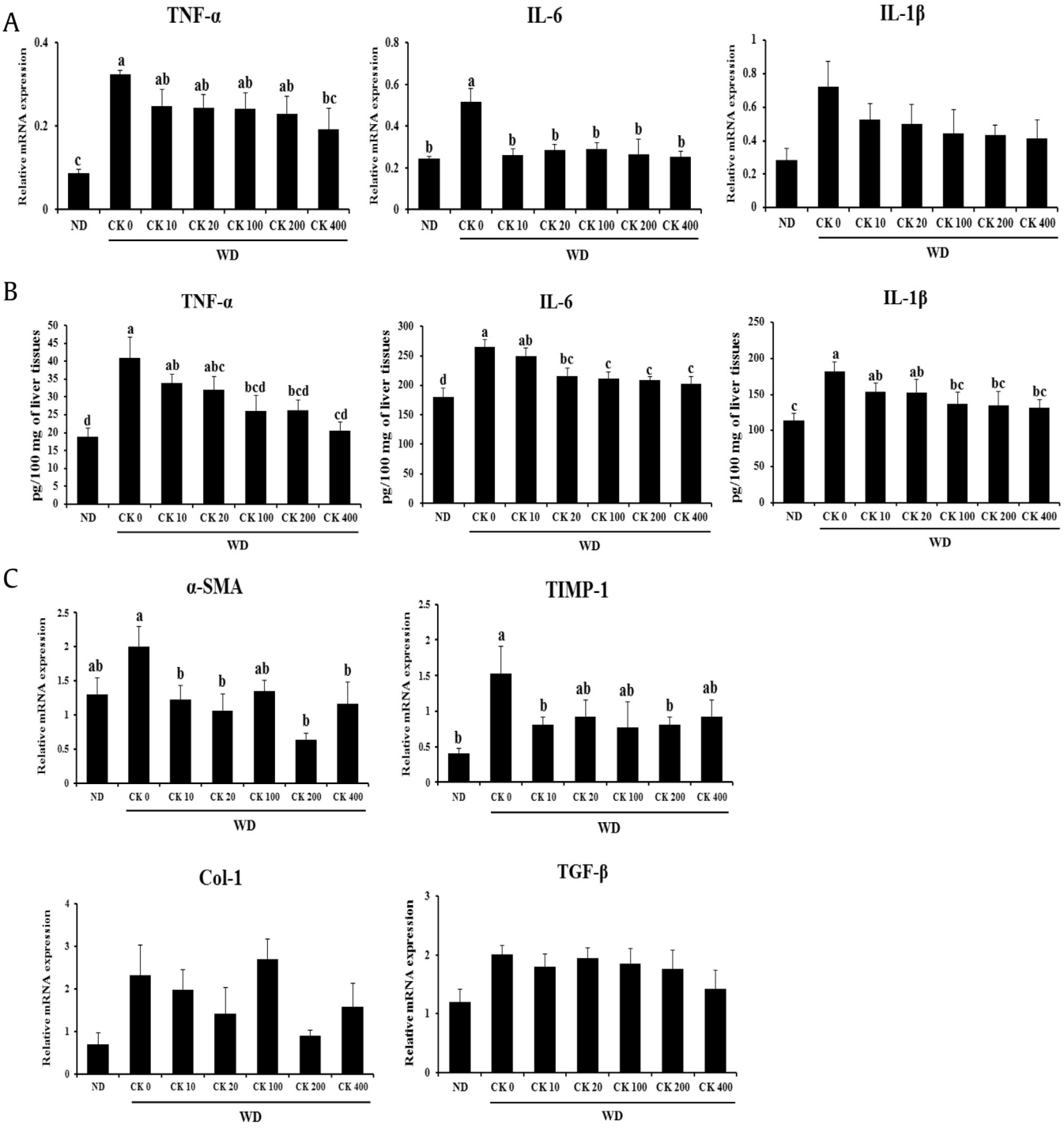

Fig. 3. Administration of GBCK25 downregulates the expression of NASH-related inflammatory or fibrogenic genes. (A) Hepatic mRNA levels and (B) protein levels of proinflammatory cytokines in the livers each group. (C) Hepatic mRNA levels of Col 1, α-SMA, TGF-β, and TIMP-1 were assessed by qRT-PCR. Statistically significant difference between groups is indicated with different letters (mean ± SEM, ANOVA, $p < 0.05$). α-SMA, alpha smooth muscle actin; ANOVA, analysis of variance; CK, compound K; IL-6, interleukin-6; IL-1β, interleukin-1 beta; NAFLD, nonalcoholic fatty liver disease; NASH, nonalcoholic steatohepatitis; ND, normal diet; qRT-PCR, quantitative real time-polymerase chain reaction; SEM, standard error of the mean; TGF-β, transforming growth factor; TIMP-1, tissue inhibitor of metalloproteinase-1; TNF-α, tumor necrosis factor-alpha; WD, Western diet.

2.14. Statistical analyses

All graphical figures were presented as means ± standard errors. Statistical significance between multiple groups was evaluated using one-way analysis of variance using SAS version 9.1 (SAS Institute Inc., Cary, NC, USA); individual comparisons were analyzed by Duncan's multiple range test. A p value < 0.05 was considered to be statistically significant.

3. Results

3.1. GBCK25 treatment ameliorates WD-induced liver injury

To elucidate whether GBCK25 administration has an impact on the development of WD-induced NASH, 6-wk-old mice were fed an ND or a WD with or without oral administration of GBCK25 (10 mg/kg/d, 20 mg/kg/d, 100 mg/kg/d, 200 mg/kg/d, or 400 mg/kg/d) for

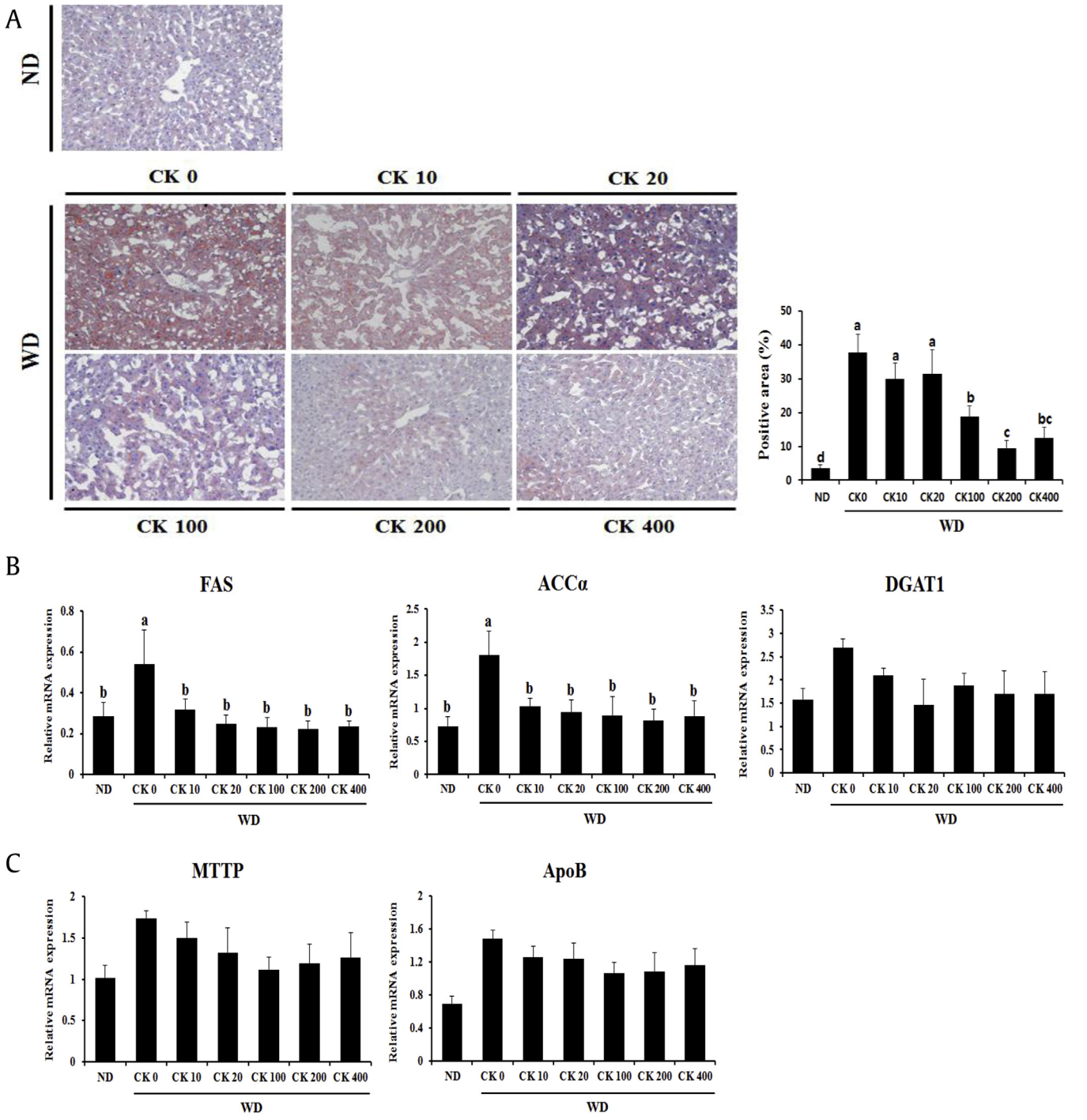

Fig. 4. Treatment of GBCK25 decreases hepatic lipid accumulation in WD-fed mice. (A) To investigate hepatic steatosis, liver tissue sections from each group were subjected to Oil Red O staining. Pictures are shown at 200× magnification. Oil Red O-positive area was determined by using an image analysis system. (B) Representative pictures showed mRNA expression levels of genes related with lipogenesis. (C) Hepatic mRNA expression of VLDL synthesis/export-related genes was determined. (D) The expression levels of fatty acid oxidation-related genes were evaluated by using qRT-PCR. (E) Representative pictures showed protein levels of CYP2E1 determined by using Western blot analysis and relative protein expression was evaluated ($n = 3$). Statistically significant difference between groups is indicated with different letters (mean ± SEM, ANOVA, $p < 0.05$). ACCα, acetyl CoA carboxylase α; ANOVA, analysis of variance; CK, compound K; CYP2E1, cytochrome P450 2E1; DGAT1, diacylglycerol *O*-acyltransferase 1; FAS, fatty acid synthase; ND, normal diet; qRT-PCR, quantitative real time-polymerase chain reaction; SEM, standard error of the mean; VLDL, very-low-density lipoprotein; WD, Western diet.

12 wks. The average food and water intake was similar in each diet group irrespective of GBCK25 administration (data not shown). To verify the role of GBCK25 on NASH severity, liver sections were stained with H&E. Decreased hepatocellular fat accumulation and lobular inflammation were observed in WD-fed mice administered with GBCK25 (Fig. 2A). WD-fed mice showed increased body weight compared to ND-fed mice. However, statistical difference was not observed in body weight between WD-fed mice with or without GBCK25. Liver weight was increased in WD-fed mice compared to ND-fed mice and was significantly decreased in some GBCK25 groups of WD-fed mice, but there was no dose-dependent effect (Fig. 2B). To further determine the effects of GBCK25 on NASH severity, histopathologic observation using NAS and serum hepatic enzyme activity was performed. As shown in Fig. 2C, NAS, as

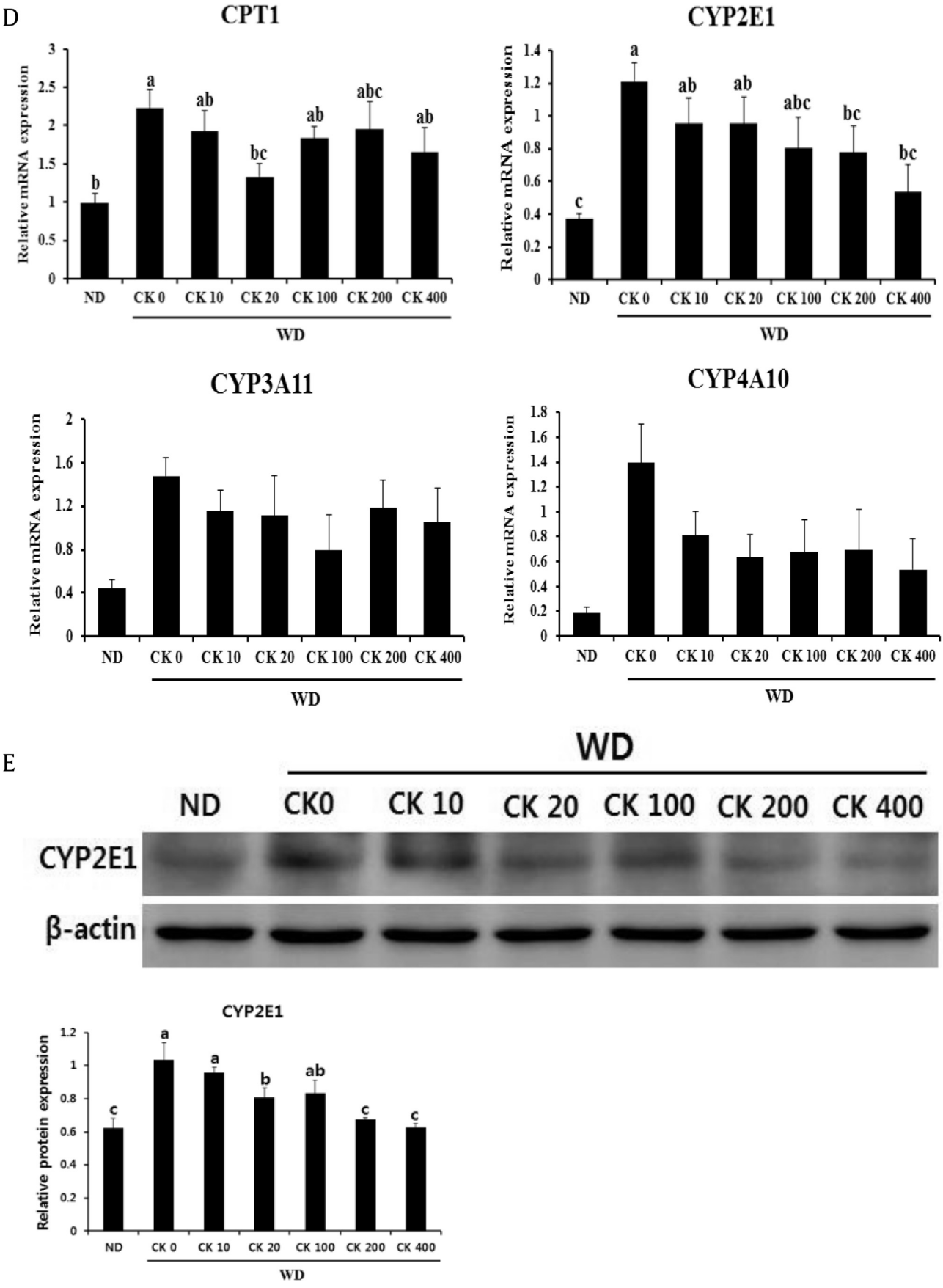

Fig. 4. (*continued*).

determined by the degree of steatosis, inflammation, and ballooning degeneration, was significantly lower in WD-fed mice administered with GBCK25 regardless of GBCK25 concentration compared to WD-fed mice. Also, serum ALT was significantly decreased by GBCK25 administration (Fig. 2D). However, serum AST levels were slightly, but not significantly, decreased in GBCK25-administered, WD-fed mice except for the GBCK25 dose of 200 mg/kg/d. In accordance with the histopathologic observation, hepatic TC and TG levels were significantly decreased in WD-fed mice with GBCK25 administration in a dose-dependent manner (Fig. 2D). Overall, these results indicate that NASH-induced liver injury was diminished by GBCK25 intake.

3.2. Administration of GBCK25 affects NASH-related inflammation and fibrosis

To investigate the effect of GBCK25 on inflammatory and fibrogenic responses, the mRNA levels of hepatic genes related to inflammatory and fibrogenic responses were determined using qRT-PCR. The mRNA levels of tissue TNF-α were significantly downregulated in the liver tissue of WD-fed mice receiving the high dose of GBCK25 compared to WD-fed mice (Fig. 3A). Hepatic mRNA levels of IL-6 were markedly decreased in WD-fed mice administered all concentrations of GBCK25. These were not observed in hepatic mRNA levels of IL-1β. However, protein levels of these inflammatory cytokines were significantly decreased in the liver tissue of WD-fed mice receiving the high dose of GBCK25 compared to WD-fed mice (Fig. 3B). In line with decreased NASH-related inflammation via treatment of GBCK25, significantly decreased hepatic mRNA levels of alpha smooth muscle actin and tissue inhibitor of metalloproteinase-1 (TIMP-1) were observed in some groups of GBCK25-administered, WD-fed mice compared to WD-fed mice. However, the mRNA levels of type I collagen alpha 1 and transforming growth factor-beta did not differ between these groups (Fig. 3C). Although WD-fed mice displayed mild inflammation and fibrosis, the data indicate that administration of GBCK25 ameliorated NASH-related inflammation and fibrosis in mice.

3.3. Administration of GBCK25 decreases hepatocellular lipid accumulation induced by WD feeding

To evaluate whether GBCK25 administration has an impact on hepatic steatosis, we first performed Oil Red O staining in liver tissue sections and then quantified the Oil Red O-positive area. Increased hepatocellular fat deposition was observed in the liver sections of WD-fed mice than those of ND-fed mice. Such lesions were significantly decreased in GBCK25-administered, WD-fed mice (Fig. 4A). Next, we evaluated the hepatic mRNA levels of *de novo* lipogenesis-associated genes including fatty acid synthase (FAS), acetyl CoA carboxylase α (ACCα), and diacylglycerol *O*-acyltransferase 1 (DGAT1). Significantly decreased levels of FAS and ACCα, but not DGAT1, were observed in GBCK25-administered, WD-fed mice compared to WD-fed mice (Fig. 4B).

Because intrahepatic TG is either stored or released in combination with very-low-density lipoprotein (VLDL) particles [30], we examined the VLDL synthesis/export-related genes such as microsomal TG transfer protein (MTP) and apolipoprotein B (ApoB). No significant differences were evident between the groups (Fig. 4C). Finally, we measured the fatty acid oxidation-related genes carnitine palmitoyltransferase 1 (CPT1), CYP2E1, CYP3A11, and CYP4A10. Hepatic expression levels of CYP2E1 were significantly decreased in GBCK25-administered, WD-fed mice in a dose-dependent manner (Fig. 4D). This finding was further supported by Western blot analysis showing significant reduction of CYP2E1 protein levels in the livers of GBCK25-treated mice (Fig. 4E). Taken together, these findings indicate that administration of GBCK25 diminished hepatic lipid accumulation in the WD-induced NASH model.

3.4. Administration of GBCK25 decreases hepatocellular oxidative stress and JNK activation

Because lipid peroxidation and its associated lipotoxic cellular damage are involved in the pathogenesis of NASH [31], we evaluated the levels of lipid peroxidation by measuring MDA. Increased hepatic MDA levels induced by WD feeding were abrogated in WD-fed mice administered with GBSK25 (Fig. 5A). To further explore the role of GBCK25 on lipid peroxidation-mediated hepatocellular damage, we determined whether GBCK25 administration affects JNK activation (phosphorylation) because of its role in hepatocellular lipoapoptosis induced by free fatty acids (FFAs) [32]. JNK activation was increased in the livers of WD-fed mice compared to ND-fed mice. This activation was decreased by GBCK25 administration (Fig. 5B), indicating that decreased CYP2E1-mediated lipid peroxidation is closely associated with cellular JNK pathway leading to cellular damage. Overall, these findings indicate that GBCK25 has protective activity against NASH-associated lipotoxicity in mice.

3.5. Treatment with GBCK25 attenuates oxidative activity and hepatic inflammation in vitro

To more clearly demonstrate the effects of GBCK25 on NASH-related hepatocellular damage and inflammation, *in vitro* experiments were performed using AML12 or RAW 264.7 cells with or without PA or LPS stimulation, respectively. After determining the concentration of GBCK25 without cytotoxicity in AML12 cells (Fig. 6A), the effect of GBCK25 on cellular damage and lipid accumulation were assessed in PA-treated AML12 cells. Decreased cytotoxic effect and cellular TG levels were observed in PA-treated AML12 cells with GBCK25 treatment (Fig. 6B). In line with reduction of cellular TG levels combined with *in vivo* results, GBCK25 treatment significantly decreased the mRNA expression levels of lipogenic FAS and ACCα. The effects were also observed in the mRNA expression levels of CYP2E1 (Fig. 6C), indicating that GBCK25 reduced hepatic steatosis and CYP2E1-mediated oxidative stress, and consequently decreased NASH severity. These findings were further supported by Western blot analysis, showing that protein levels of CYP2E1 and pJNK were decreased in PA-treated AML12 cells with GBCK25 treatment (Fig. 6D). These results suggest that GBCK25 has antisteatotic effects and antioxidative activity via reducing CYP2E1 and JNK activation leading to hepatocellular lipotoxic damage. Finally, we investigated whether GBCK25 treatment affected inflammatory responses. After determining the concentration of GBCK25 without cytotoxicity in RAW264.7 cells and primary KCs (Fig. 6E), mRNA expression levels of proinflammatory genes were significantly decreased by treatment of GBCK25 in LPS-treated RAW264.7 cells (Fig. 6F) and primary KCs (Fig. 6G). Taken together, these results combined with findings from our *in vivo* experiments suggest that GBCK25 ameliorates NASH severity by affecting lipid accumulation, oxidative stress-mediated cellular damage, and inflammation.

4. Discussion

Recently, there has been a growing concern about the increasing prevalence of NAFLD and its associated complications. NASH is one of the common forms of chronic and severe liver disorders worldwide. Because its incidence has risen steadily in obese people, many studies have been undertaken to try to elucidate the exact mechanism of progression from steatosis and steatohepatitis,

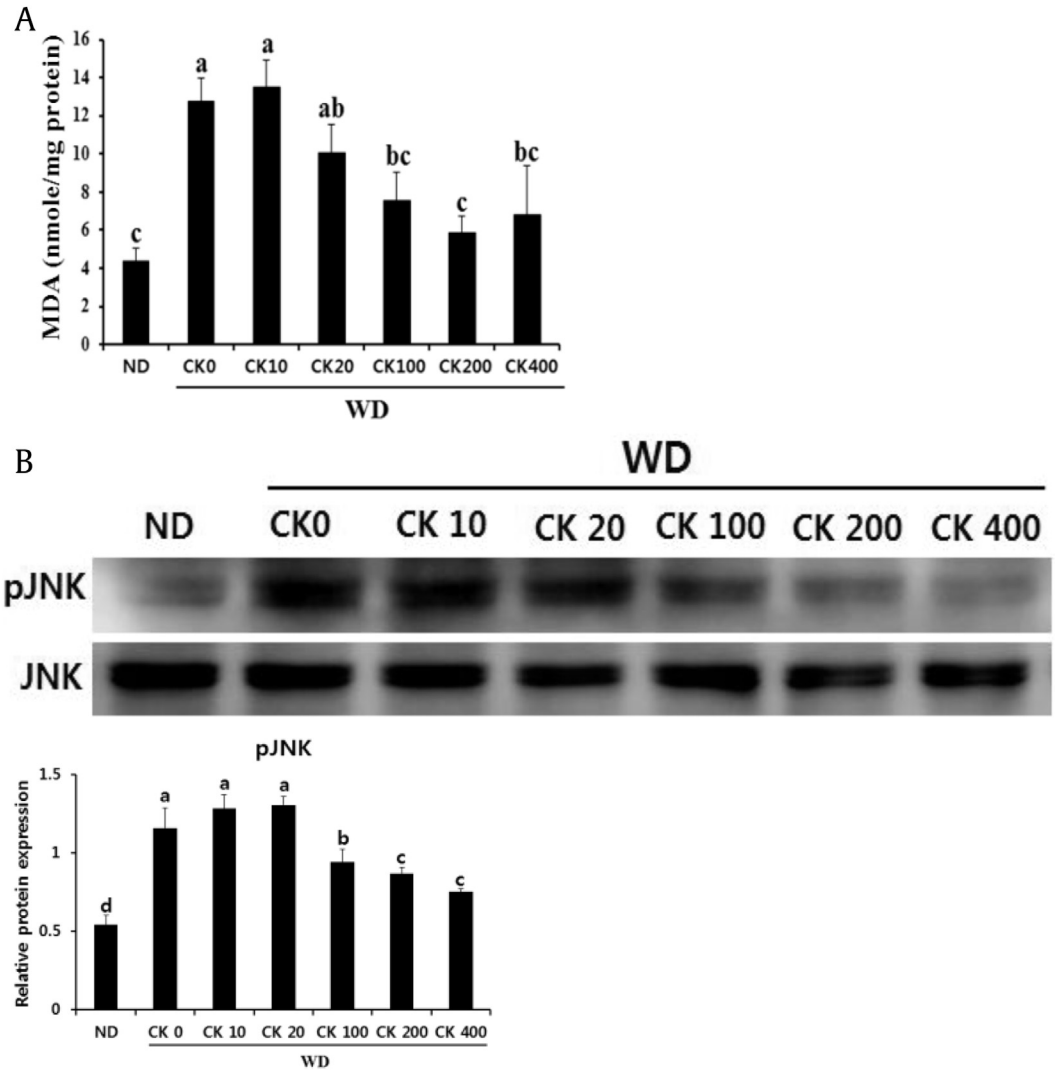

Fig. 5. Administration of GBCK25 reduces hepatic lipid peroxidation and JNK phosphorylation. (A) In order to assess lipid peroxidation, MDA was measured in the livers of each group. (B) Representative pictures showed protein levels of pJNK and JNK as determined by using Western blot analysis and relative protein expression was evaluated ($n = 3$). Statistically significant difference between groups is indicated with different letters (mean ± SEM, ANOVA, $p < 0.05$). ANOVA, analysis of variance; CK, compound K; JNK, c-Jun N-terminal kinase; MDA, malondialdehyde; NC, negative control; pJNK, phospho JNK; SEM, standard error of the mean; WD, Western diet.

without definitive success. Several experimental rodent models of NASH were proposed to mimic human NASH. Of these, spontaneous NASH caused by genetic mutation has been proposed. Also, another well-documented NASH model is nonspontaneous NASH induced by dietary or pharmacological manipulation. Among these, the methionine-choline deficient (MCD) diet is a widely used and well-accepted diet model to induce NASH. However, MCD diet-induced NASH differs markedly from human NASH because mice fed MCD diet showed low plasma TG levels and histological difference of hepatic steatosis as well as remarkable weight loss [33].

In seeking to overcome these problems of MCD diet-induced NASH, a recent study described that mice fed a diet high in fat (36%) and sucrose (30%) for 15 wks displayed hepatocellular lipid accumulation with mild inflammation and fibrosis compared to HFD-fed mice [34]. This finding was further supported by another study indicating diet-induced steatosis via a fructokinase-dependent pathway [35]. Because free cholesterol (FC) accumulation in hepatic stellate cells plays a pivotal role in the progression of NASH-related fibrosis [36], we herein used a 12-wk NASH model induced by Western-style diet containing high cholesterol. However, mild hepatic inflammatory and fibrogenic responses were observed in WD-fed mice compared to ND-fed mice. Based on a previous study that used a 24-wk diet high in fat and cholesterol [36], a possible reason for our observations of mild inflammation and fibrosis is that the length of the diet was not enough to fully induce inflammatory and fibrogenic responses. Furthermore, a recent study reported that WD-fed mice showed different NASH phenotype depending on mouse strain; lower NASH-related fibrosis was observed in C57BL/6 mouse when compared to other mouse strains [37]. Similar to this result, there was no significant difference of collagen deposition between ND-fed mice and WD-fed, mice as confirmed by Sirius-red staining in our study (data not shown).

Based on the “two-hit” theory explaining the pathogenesis of NASH proposed by Day et al. [38], oxidative stress-mediated lipid peroxidation and mitochondrial dysfunction can act as second trigger to promote the progression from steatosis to steatohepatitis. CYP2E1 is a member of the cytochrome P450 family and can oxidize several molecules including ethanol and fatty acids. Therefore, increased CYP2E1 activity is closely associated with generation of ROS leading to microsomal lipid peroxidation resulting in cellular oxidative damages [2]. In accordance with this finding, increased CYP2E1 expression and its associated lipid peroxidation were observed in both NASH patients and animal models of NASH [39–

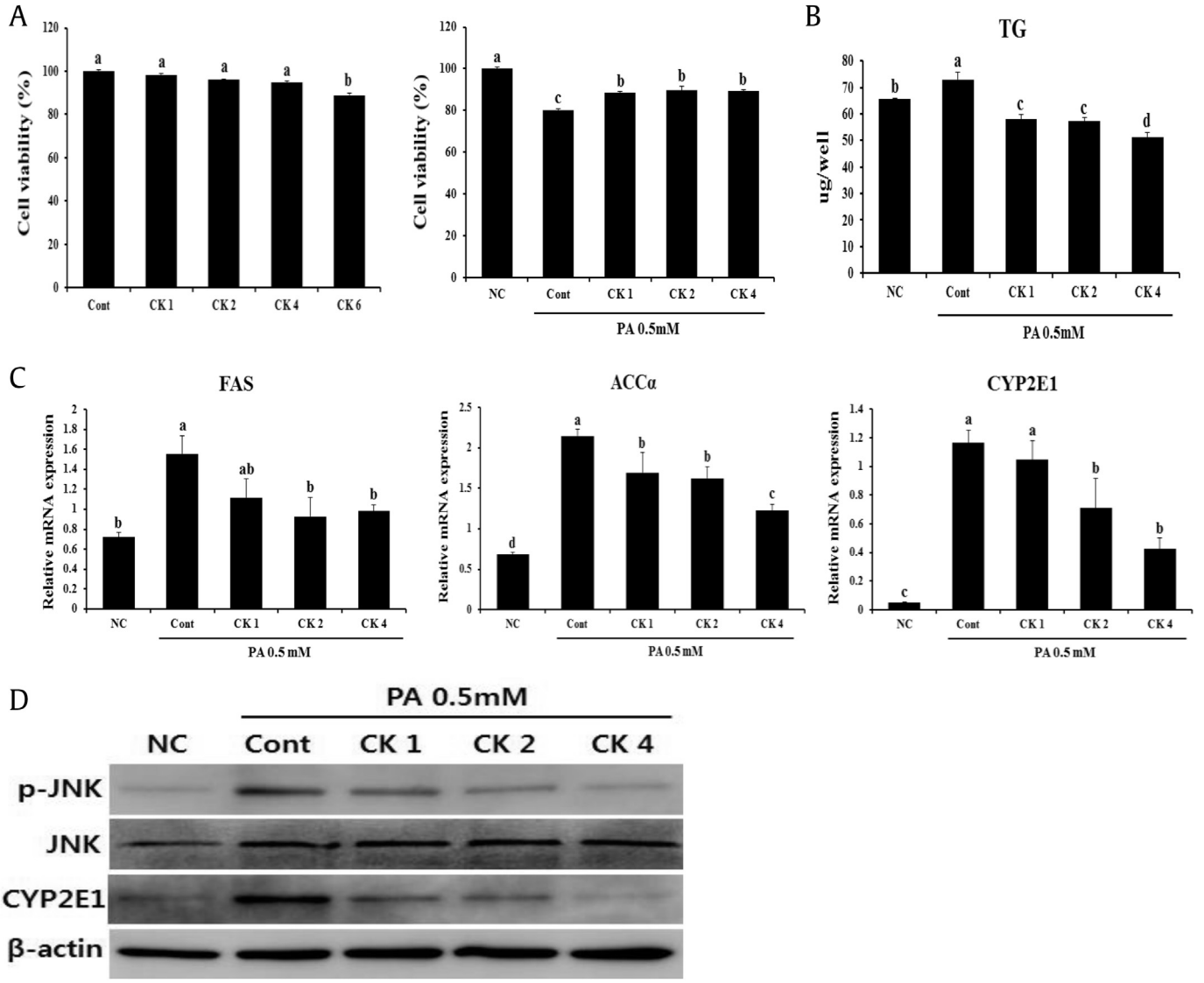

Fig. 6. GBCK25 treatment alleviates NASH-related cytotoxicity and inflammation. (A) AML12 cells treated with various concentrations of GBCK25 were incubated for 24 h, and then cell cytotoxicity was determined by the MTS assay. (B) The effects of GBCK25 on cellular toxicity were determined in PA-treated AML12 cells by MTS assay and lipid accumulation was determined by measurement of TG. (C) Hepatic mRNA expressions of lipogenesis-related genes and CYP2E1 were determined using qRT-PCR. (D) Representative pictures show protein levels of CYP2E1, pJNK, JNK, and β-actin determined using Western blot analysis. (E) The viability of RAW264.7 cells and primary KCs were evaluated in the same method as described above. The effects of GBCK25 on inflammation in LPS-treated (F) RAW264.7 cells and (G) primary KCs as determined by qRT-PCR. Statistically significant difference between groups is indicated with different letters (mean ± SEM, ANOVA, $p < 0.05$). ACCα, acetyl CoA carboxylase α; AML12, alpha mouse liver 12; ANOVA, analysis of variance; CK, compound K; Cont, control; CYP2E1, cytochrome P450 2E1; FAS, fatty acid synthase; IL-6, interleukin-6; IL-1β, interleukin-1 beta; JNK, c-Jun N-terminal kinase; KC, Kupffer cells; LPS, lipopolysaccharide; MDA, malondialdehyde; NC, negative control; PA, palmitic acid; pJNK, phospho JNK; qRT-PCR, quantitative real time-polymerase chain reaction; SEM, standard error of the mean; TG, triglyceride; TNF-α, tumor necrosis factor-alpha.

41]. Thus, several studies have been conducted to identify the effects of CYP2E1 on the pathogenesis of NAFLD and/or NASH through the genetic manipulation of CYP2E1. Hepatocyte-specific overexpression of CYP2E1 was involved in increased IR partially mediated by the JNK pathway [42]. Also, reduced NASH severity was observed in CYP2E1-deficient mice owing to decreased oxidative/nitrosative stress, inflammation, fibrosis, and IR [43,44]. Consistent with this finding, similar results were observed in CYP2E1-deficient mice with ethanol feeding [45]. Also, these mice showed decreased aging-related steatosis, apoptosis, and fibrosis through reducing nitroxidative stress, providing important roles of CYP2E1 on the pathogenesis of aging-related liver diseases [46].

Growing evidence has strongly indicated that hepatic CYP2E1 is critical in the oxidative stress-mediated cell death induced by ethanol or acetaminophen overdose through JNK activation [47–49]. Also, activation of JNK was notably decreased in CYP2E1-deficient mice fed with HFD compared to that of wild-type mice [43]. Furthermore, dysregulation of CYP2E1 degradation leads to continued and increased cellular oxidative stress and JNK activation, which results in increased NASH severity. Consistent with these findings, GBCK25 administration significantly downregulated hepatic CYP2E1 *in vitro* and *in vivo* in the present study with concomitantly decreased oxidative stress and JNK activation in steatohepatitic livers. These results were further supported by

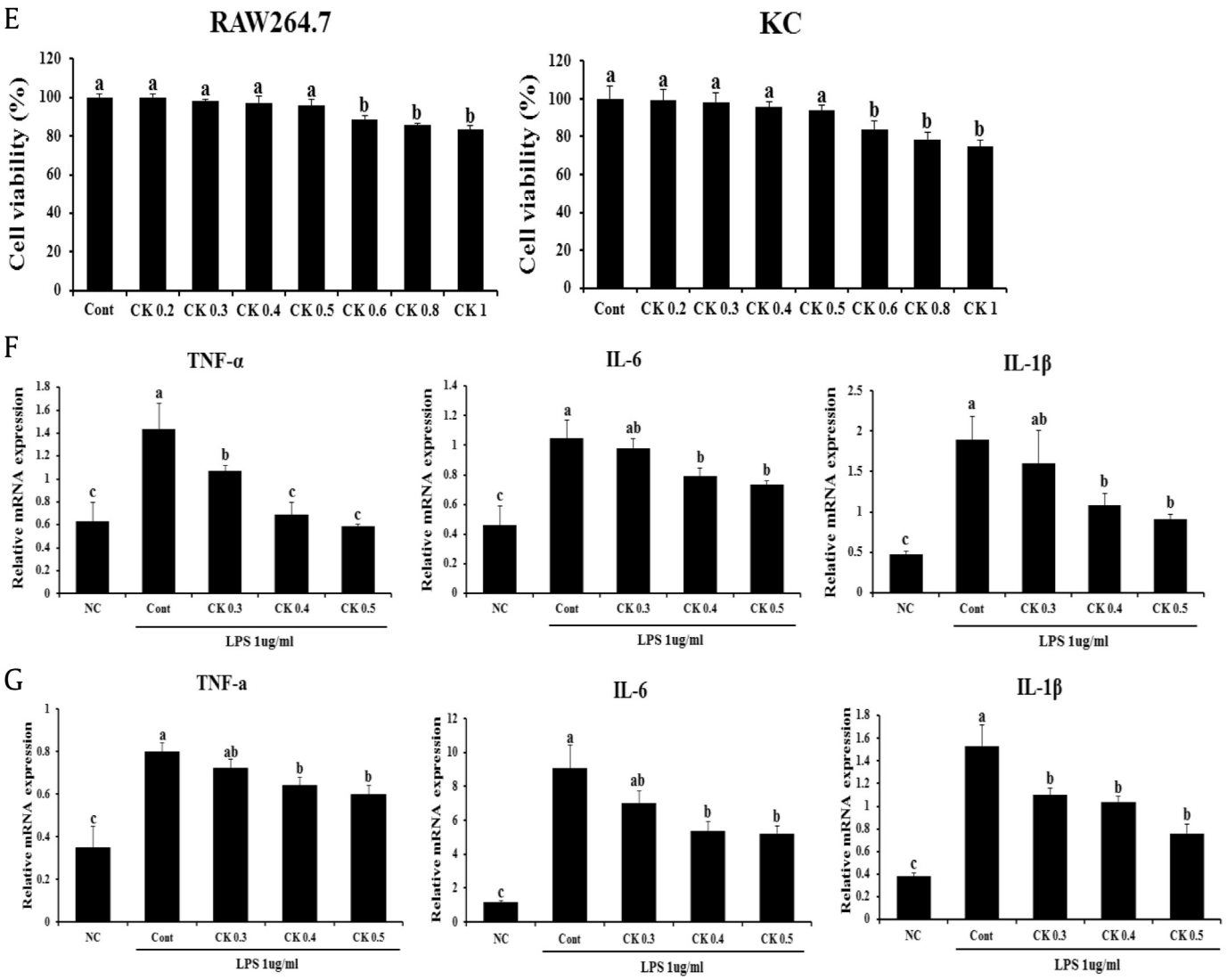

Fig. 6. (*continued*).

recent studies showing that ginseng or its components including saponins also abrogated CYP2E1 induction, thereby reducing acetaminophen- or ethanol-mediated oxidative stress, inflammation, and hepatotoxicity [50,51]. Although CYP2E1 is the major enzyme responsible for microsomal lipid peroxidation in steatohepatitic livers, CYP2E1-deficient mice still develop diet-induced NASH and its associated lipid peroxidation [41]. Thus, CYP2E1-independent and another enzyme-mediated pathway might be responsible for lipid peroxidation in steatohepatitic livers. Notably, expression levels of CYP4A10 and CYP4A14 were significantly increased in CYP2E1-deficient mice with NASH, and inhibition of CYP4A10 abrogated hepatic microsomal lipid peroxidation [41], indicating the important role of CYP4A10 on the pathogenesis of NASH and its associated lipid peroxidation. However, GBCK25 administration in the present study did not affect the mRNA levels of CYP4A10 in WD-fed mice. Therefore, we conclude that decreased lipid peroxidation by GBCK25 administration is closely associated with reduced levels of CYP2E1, but not CYP4A10.

Elevated serum level of FFA is one of the features of NAFLD/NASH, and FFA accumulation accelerates hepatocellular cytotoxic damage by affecting proapoptotic proteins, such as Bax, and activating JNK [52]. A recent study indicated that FC accumulation in hepatocytes triggers mitochondrial injury and subsequent induction of FC-mediated hepatocellular lipotoxicity through JNK1 activation. High-mobility-group-box 1 (HMGB1) released from these necrotic hepatocytes induced cytotoxic effects of nearby hepatocytes laden with FC through binging its receptor Toll-like receptor 4 in a paracrine-dependent manner [53]. Because ginseng and/or CK has the reducing activity of serum lipid component and antilipolytic effects in adipocytes resulting in decreased serum levels of FFA and FC [54–56], the decreased JNK activation noted presently might be affected by reduced FFA and FC by GBCK25 exposure. Further experiments need to be performed to determine the levels of FFA and FC between WD-fed group and WD-fed group with GBCK25 administration. Also, we need to test whether or not GBCK25 administration abrogates hepatic JNK activation of WD-fed mice under the CYP2E1 inhibited or deficient condition to more clearly demonstrate the effects of GBCK25 on NASH severity via CYP2E1 modulation.

In conclusion, administration of GBCK25 can ameliorate diet-induced NASH severity by modulating CYP2E1-mediated lipid peroxidation and its associated JNK-mediated cellular damage.

Therefore, administration of GBCK25 could be a potentially effective prophylactic strategy and alternative therapy to prevent and/or treat metabolic diseases including NASH.

Conflicts of interest

The authors declare that there are no conflicts of interest.

Acknowledgments

This research was supported by the Ministry of Trade, Industry & Energy (MOTIE), Korea Institute for Advancement of Technology (KIAT) through the Encouragement Program for The Industries of Economic Cooperation Region (R0004537).

References

[1] Roberts EA. Nonalcoholic steatohepatitis in children. Curr Gastroenterol Rep 2003;5:253–9.
[2] Aubert J, Begriche K, Knockaert L, Robin MA, Fromenty B. Increased expression of cytochrome P450 2E1 in nonalcoholic fatty liver disease: mechanisms and pathophysiological role. Clin Res Hepatol Gastroenterol 2011;35:630–7.
[3] Bellentani S, Bedogni G, Tiribelli C. Liver and heart: a new link? J Hepatol 2008;49:300–2.
[4] Ratziu V, Voiculescu M, Poynard T. Touching some firm ground in the epidemiology of NASH. J Hepatol 2012;56:23–5.
[5] Begriche K, Igoudjil A, Pessayre D, Fromenty B. Mitochondrial dysfunction in NASH: causes, consequences and possible means to prevent it. Mitochondrion 2006;6:1–28.
[6] Anstee QM, Daly AK, Day CP. Genetics of alcoholic and nonalcoholic fatty liver disease. Semin Liver Dis 2011;31:128–46.
[7] Dhar SK, St Clair DK. Manganese superoxide dismutase regulation and cancer. Free Radic Biol Med 2012;52:2209–22.
[8] Crawford A, Fassett RG, Geraghty DP, Kunde DA, Ball MJ, Robertson IK, Coombes JS. Relationships between single nucleotide polymorphisms of antioxidant enzymes and disease. Gene 2012;501:89–103.
[9] Wu CW, Yu J. Molecular basis for a functional role of cytochrome P450 2E1 in non-alcoholic steatohepatitis. J Gastroenterol Hepatol 2010;25:1019–20.
[10] Leung TM, Nieto N. CYP2E1 and oxidant stress in alcoholic and non-alcoholic fatty liver disease. J Hepatol 2013;58:395–8.
[11] Gonzalez FJ. Role of cytochromes P450 in chemical toxicity and oxidative stress: studies with CYP2E1. Mutat Res 2005;569:101–10.
[12] Yu MW, Gladek-Yarborough A, Chiamprasert S, Santella RM, Liaw YF, Chen CJ. Cytochrome P450 2E1 and glutathione *S*-transferase M1 polymorphisms and susceptibility to hepatocellular carcinoma. Gastroenterology 1995;109:1266–73.
[13] Huang YS, Chern HD, Su WJ, Wu JC, Chang SC, Chiang CH, Chang FY, Lee SD. Cytochrome P450 2E1 genotype and the susceptibility to antituberculosis drug-induced hepatitis. Hepatology 2003;37:924–30.
[14] Varela NM, Quinones LA, Orellana M, Poniachik J, Csendes A, Smok G, Rodrigo R, Caceres DD, Videla LA. Study of cytochrome P450 2E1 and its allele variants in liver injury of nondiabetic, nonalcoholic steatohepatitis obese women. Biol Res 2008;41:81–92.
[15] Piao YF, Li JT, Shi Y. Relationship between genetic polymorphism of cytochrome P450IIE1 and fatty liver. World J Gastroenterol 2003;9:2612–5.
[16] Cho IH. Effects of *Panax ginseng* in neurodegenerative diseases. J Ginseng Res 2012;36:342–53.
[17] Dai D, Zhang CF, Williams S, Yuan CS, Wang CZ. Ginseng on cancer: potential role in modulating inflammation-mediated angiogenesis. Am J Chin Med 2017;45:13–22.
[18] Hong M, Lee YH, Kim S, Suk KT, Bang CS, Yoon JH, Baik GH, Kim DJ, Kim MJ. Anti-inflammatory and antifatigue effect of Korean Red Ginseng in patients with nonalcoholic fatty liver disease. J Ginseng Res 2016;40:203–10.
[19] Hong SH, Suk KT, Choi SH, Lee JW, Sung HT, Kim CH, Kim EJ, Kim MJ, Han SH, Kim MY, et al. Anti-oxidant and natural killer cell activity of Korean red ginseng (*Panax ginseng*) and urushiol (*Rhus vernicifera* Stokes) on non-alcoholic fatty liver disease of rat. Food Chem Toxicol 2013;55:586–91.
[20] Liu Y, Hao F, Zhang H, Cao D, Lu X, Li X. *Panax notoginseng* saponins promote endothelial progenitor cell mobilization and attenuate atherosclerotic lesions in apolipoprotein E knockout mice. Cell Physiol Biochem 2013;32:814–26.
[21] Ming Y, Chen Z, Chen L, Lin D, Tong Q, Zheng Z, Song G. Ginsenoside compound K attenuates metastatic growth of hepatocellular carcinoma, which is associated with the translocation of nuclear factor-kappaB p65 and reduction of matrix metalloproteinase-2/9. Planta Med 2011;77:428–33.
[22] Igami K, Shimojo Y, Ito H, Miyazaki T, Kashiwada Y. Hepatoprotective effect of fermented ginseng and its major constituent compound K in a rat model of paracetamol (acetaminophen)-induced liver injury. J Pharm Pharmacol 2015;67:565–72.
[23] Lee HU, Bae EA, Han MJ, Kim NJ, Kim DH. Hepatoprotective effect of ginsenoside Rb1 and compound K on tert-butyl hydroperoxide-induced liver injury. Liver Int 2005;25:1069–73.
[24] Kim DY, Yuan HD, Chung IK, Chung SH. Compound K, intestinal metabolite of ginsenoside, attenuates hepatic lipid accumulation via AMPK activation in human hepatoma cells. J Agric Food Chem 2009;57:1532–7.
[25] Wei S, Li W, Yu Y, Yao F, A L, Lan X, Guan F, Zhang M, Chen L. Ginsenoside compound K suppresses the hepatic gluconeogenesis via activating adenosine-5′ monophosphate kinase: a study in vitro and in vivo. Life Sci 2015;139:8–15.
[26] Kim MS, Lee KT, Iseli YJ, Hoy AJ, George J, Grewal T, Roufogalis BD. Compound K modulates fatty acid-induced lipid droplet formation and expression of proteins involved in lipid metabolism in hepatocytes. Liver Int 2013;33:1583–93.
[27] Chen XJ, Liu WJ, Wen ML, Liang H, Wu SM, Zhu YZ, Zhao JY, Dong XQ, Li MG, Bian L, et al. Ameliorative effects of compound K and ginsenoside Rh1 on non-alcoholic fatty liver disease in rats. Sci Rep 2017;7:41144.
[28] Kleiner DE, Brunt EM, Van Natta M, Behling C, Contos MJ, Cummings OW, Ferrell LD, Liu YC, Torbenson MS, Unalp-Arida R, et al. Design and validation of a histological scoring system for nonalcoholic fatty liver disease. Hepatology 2005;41:1313–21.
[29] Roh YS, Park S, Kim JW, Lim CW, Seki E, Kim B. Toll-like receptor 7-mediated type I interferon signaling prevents cholestasis- and hepatotoxin-induced liver fibrosis. Hepatology 2014;60:237–49.
[30] Browning JD, Horton JD. Molecular mediators of hepatic steatosis and liver injury. J Clin Invest 2004;114:147–52.
[31] Akazawa Y, Nakao K. Lipotoxicity pathways intersect in hepatocytes: endoplasmic reticulum stress, c-Jun N-terminal kinase-1, and death receptors. Hepatol Res 2016;46:977–84.
[32] Cazanave SC, Mott JL, Elmi NA, Bronk SF, Werneburg NW, Akazawa Y, Kahraman A, Garrison SP, Zambetti GP, Charlton MR, et al. JNK1-dependent PUMA expression contributes to hepatocyte lipoapoptosis. J Biol Chem 2009;284:26591–602.
[33] Anstee QM, Goldin RD. Mouse models in non-alcoholic fatty liver disease and steatohepatitis research. Int J Exp Pathol 2006;87:1–16.
[34] Ishimoto T, Lanaspa MA, Rivard CJ, Roncal-Jimenez CA, Orlicky DJ, Cicerchi C, McMahan RH, Abdelmalek MF, Rosen HR, Jackman MR, et al. High-fat and high-sucrose (western) diet induces steatohepatitis that is dependent on fructokinase. Hepatology 2013;58:1632–43.
[35] Ishimoto T, Lanaspa MA, Le MT, Garcia GE, Diggle CP, Maclean PS, Jackman MR, Asipu A, Roncal-Jimenez CA, Kosugi T, et al. Opposing effects of fructokinase C and A isoforms on fructose-induced metabolic syndrome in mice. Proc Natl Acad Sci USA 2012;109:4320–5.
[36] Tomita K, Teratani T, Suzuki T, Shimizu M, Sato H, Narimatsu K, Okada Y, Kurihara C, Irie R, Yokoyama H, et al. Free cholesterol accumulation in hepatic stellate cells: mechanism of liver fibrosis aggravation in nonalcoholic steatohepatitis in mice. Hepatology 2014;59:154–69.
[37] Asgharpour A, Cazanave SC, Pacana T, Seneshaw M, Vincent R, Banini BA, Kumar DP, Daita K, Min HK, Mirshahi F, et al. A diet-induced animal model of non-alcoholic fatty liver disease and hepatocellular cancer. J Hepatol 2016;65:579–88.
[38] Day CP, James OF. Steatohepatitis: a tale of two "hitsZ"? Gastroenterology 1998;114:842–5.
[39] Weltman MD, Farrell GC, Hall P, Ingelman-Sundberg M, Liddle C. Hepatic cytochrome P450 2E1 is increased in patients with nonalcoholic steatohepatitis. Hepatology 1998;27:128–33.
[40] Leclercq IA, Farrell GC, Field J, Bell DR, Gonzalez FJ, Robertson GR. CYP2E1 and CYP4A as microsomal catalysts of lipid peroxides in murine nonalcoholic steatohepatitis. J Clin Invest 2000;105:1067–75.
[41] Sanyal AJ, Campbell-Sargent C, Mirshahi F, Rizzo WB, Contos MJ, Sterling RK, Luketic VA, Shiffman ML, Clore JN. Nonalcoholic steatohepatitis: association of insulin resistance and mitochondrial abnormalities. Gastroenterology 2001;120:1183–92.
[42] Schattenberg JM, Wang Y, Singh R, Rigoli RM, Czaja MJ. Hepatocyte CYP2E1 overexpression and steatohepatitis lead to impaired hepatic insulin signaling. J Biol Chem 2005;280:9887–94.
[43] Abdelmegeed MA, Banerjee A, Yoo SH, Jang S, Gonzalez FJ, Song BJ. Critical role of cytochrome P450 2E1 (CYP2E1) in the development of high fat-induced non-alcoholic steatohepatitis. J Hepatol 2012;57:860–6.
[44] Abdelmegeed MA, Choi Y, Godlewski G, Ha SK, Banerjee A, Jang S, Song BJ. Cytochrome P450-2E1 promotes fast food-mediated hepatic fibrosis. Sci Rep 2017;7:39764.
[45] Lu Y, Zhuge J, Wang X, Bai J, Cederbaum AI. Cytochrome P450 2E1 contributes to ethanol-induced fatty liver in mice. Hepatology 2008;47:1483–94.
[46] Abdelmegeed MA, Choi Y, Ha SK, Song BJ. Cytochrome P450-2E1 promotes aging-related hepatic steatosis, apoptosis and fibrosis through increased nitroxidative stress. Free Radic Biol Med 2016;91:188–202.
[47] Lu Y, Wu D, Wang X, Ward SC, Cederbaum AI. Chronic alcohol-induced liver injury and oxidant stress are decreased in cytochrome P4502E1 knockout mice and restored in humanized cytochrome P4502E1 knock-in mice. Free Radic Biol Med 2010;49:1406–16.
[48] Jing Y, Wu K, Liu J, Ai Q, Ge P, Dai J, Jiang R, Zhou D, Che Q, Wan J, et al. Aminotriazole alleviates acetaminophen poisoning via downregulating P450 2E1 and suppressing inflammation. PLoS One 2015;10, e0122781.
[49] Cederbaum AI, Yang L, Wang X, Wu D. CYP2E1 sensitizes the liver to LPS- and TNF alpha-induced toxicity via elevated oxidative and nitrosative stress and activation of ASK-1 and JNK mitogen-activated kinases. Int J Hepatol 2012;2012:582790.

[50] Ding RB, Tian K, Cao YW, Bao JL, Wang M, He C, Hu Y, Su H, Wan JB. Protective effect of panax notoginseng saponins on acute ethanol-induced liver injury is associated with ameliorating hepatic lipid accumulation and reducing ethanol-mediated oxidative stress. J Agric Food Chem 2015;63:2413–22.
[51] Gum SI, Cho MK. Korean red ginseng extract prevents APAP-induced hepatotoxicity through metabolic enzyme regulation: the role of ginsenoside Rg3, a protopanaxadiol. Liver Int 2013;33:1071–84.
[52] Malhi H, Gores GJ. Molecular mechanisms of lipotoxicity in nonalcoholic fatty liver disease. Semin Liver Dis 2008;28:360–9.
[53] Gan LT, Van Rooyen DM, Koina ME, McCuskey RS, Teoh NC, Farrell GC. Hepatocyte free cholesterol lipotoxicity results from JNK1-mediated mitochondrial injury and is HMGB1 and TLR4-dependent. J Hepatol 2014;61:1376–84.
[54] Wang H, Reaves LA, Edens NK. Ginseng extract inhibits lipolysis in rat adipocytes in vitro by activating phosphodiesterase 4. J Nutr 2006;136:337–42.
[55] Jiang S, Ren D, Li J, Yuan G, Li H, Xu G, Han X, Du P, An L. Effects of compound K on hyperglycemia and insulin resistance in rats with type 2 diabetes mellitus. Fitoterapia 2014;95:58–64.
[56] Kim SH, Park KS. Effects of *Panax ginseng* extract on lipid metabolism in humans. Pharmacol Res 2003;48:511–3.